The C2A Domain of Synaptotagmin Exhibits a High Binding Affinity for Copper: Implications in the Formation of the Multiprotein FGF Release Complex†

Dakshinamurthy Rajalingam,‡ Thallapuranam Krishnaswamy S. Kumar,‡ and Chin Yu*,‡,§

Department of Chemistry and Biochemistry, University of Arkansas, Fayetteville, Arkansas 72701, and Department of Chemistry, National Tsing Hua University, Hsinchu 30043, Taiwan

Received July 15, 2005; Revised Manuscript Received September 15, 2005

ABSTRACT: Human acidic fibroblast growth factor (hFGF-1) is a potent mitogen and is involved in the regulation of key cellular process such as angiogenesis, differentiation, and morphogenesis. hFGF-1 is a signal peptide-less protein that is released into the extracellular compartment as a multiprotein complex consisting of S100A13, synaptotagmin (Syt1), and a hFGF-1 homodimer. Cu^{2+} is known to play an important role in the formation of the multiprotein release complex. The source of Cu^{2+} required for the formation of the multiprotein release complex is not clear. In this study, we show that the cytoplasmic C2A domain of synaptotagmin binds to Cu^{2+} ions with high affinity. Results from the isothermal calorimetry (ITC), near-UV circular dichroism (CD), and absorption spectroscopy experiments suggest that four Cu^{2+} ions bind per molecule of C2A domain. Far-UV CD and limited trypsin digestion analysis reveal that the C2A domain undergoes a mild conformational change upon binding to Cu^{2+}. Competition experiments monitored by ITC and fluorescence resonance energy transfer indicate that Cu^{2+} and Ca^{2+} ions share common binding sites on the C2A domain. Cu^{2+} ions compete with and replace Ca^{2+} ions bound to the C2A domain. Two-dimensional nuclear magnetic resonance spectroscopy data clearly show that Cu^{2+} ions bind to the Ca^{2+} binding sites in the loops (loops 1−3) located at the apex of the structure of the C2A domain. In addition, there is a unique Cu^{2+} binding site located in the loop connecting β-strands 7 and 8. It appears that the C2A domain provides the Cu^{2+} ions required for the formation of the multiprotein FGF release complex.

Fibroblast growth factors (FGFs)[1] are ∼17 kDa all-β-sheet proteins that play crucial roles in the regulation of key cellular process such as angiogenesis, morphogenesis, wound healing, and tumor growth (*1*−*4*). Interestingly, prototype FGFs such as FGF-1 and FGF-2 lack the N-terminal peptide sequence which allows proteins to be released through the secretory pathway mediated by the endoplasmic reticulum and Golgi apparatus (*5*). FGFs are required to be released into the extracellular compartment to exhibit their biological functions by specifically binding to their cell surface receptors (*6*−*9*). Although the precise mechanism underlying the release of the signal peptide-less proteins (like FGF) is still not completely understood, recent studies by Maciag and coworkers have provided useful insights into the secretion of FGF into the extracellular compartment (*10*−*12*). Jackson et al. (*13*) demonstrated that the release of FGF-1 in response to heat shock and hypoxia requires the formation of the Cys30-mediated FGF-1 homodimer. The homodimer of FGF-1 is biologically inactive, and formation of the dimer is believed to be a mechanism of storing and transporting FGF-1 in an inactive form (*10*, *11*). Copper (Cu^{2+}) is shown to be essential for the formation of the FGF-1 homodimer because treatment with tetrathiomolybdate, a copper chelator, decreased the rate of heat shock-induced release of FGF-1 in a dose-dependent manner (*14*). FGF-1 is released under stress conditions as a component of a multiprotein aggregate containing S100A13, a calcium binding protein, and the p40 extravesicular domain of p65 synaptotagamin (p40Syt1) (*10*).

Synaptotagmins constitute a family of vesicle membrane proteins that are characterized by a short intravesicular N-terminus, a single transmembrane region, and a larger cytoplasmic region that contains calcium binding C2 domains, designated as C2A and C2B (*15*−*19*). p40Syt1 is believed to be generated by proteolytic cleavage of p65 near its transmembrane domain (*20*, *21*). p40Syt1 does not contain the signal peptide sequence and exhibits a diffuse cytosolic distribution (*10*, *11*). Both p40Syt1 and S100A13 have been shown to be indispensable for the release of FGF-1 into the extracellular compartment (*10*). In this context, it would be worthwhile to note that both S100A13 and p40Syt1 are released from cells under normal cell culture conditions (*11*).

The stress-induced Cu^{2+}-dependent assembly of the FGF-1 multiprotein release complex is mandatory for the nonclassical export of FGF-1 (*12*). Interestingly, the source of Cu^{2+} ions required for FGF-1 multiprotein assembly is still not known. The results of this study for the first time reveal that

† This study was supported in part by grants from the National Institutes of Health (NIH NCRR COBRE 1 P20 RR15569), Department of Energy (DE-FGO2-01ER15161), and the National Science Council, Taiwan.

* To whom all correspondence should be addressed. E-mail: cyu@uark.edu. Fax: (479) 575-4049. Phone: (479) 575-5646.

‡ University of Arkansas.

§ National Tsing Hua University.

[1] Abbreviations: ITC, isothermal calorimetry; HSQC, heteronuclear single-quantum coherence; CD, circular dichroism; FGF, fibroblast growth factor; NMR, nuclear magnetic resonance.

10.1021/bi051387r CCC: $30.25
Published on Web 10/14/2005

the C2A domain of Syt1 has high binding affinity for Cu^{2+} ions. Cu^{2+} and Ca^{2+} ions appear to share common binding site(s) on the C2A domain. A subtle conformational change is observed to be induced in the C2A domain upon binding to Cu^{2+} ions. The C2A domain appears to provide the Cu^{2+} ions required for the formation of the FGF-1 homodimer.

MATERIALS AND METHODS

Ingredients for Luria Broth were obtained from AMRESCO. Aprotinin, pepstatin, leupeptin, phenylmethanesulfonyl fluoride, Triton X-100, terbium chloride, and β-mercaptoethanol were obtained from Sigma Co. (St. Louis, MO). Glutathione−Sepharose was obtained from Amersham Pharmacia Biotech. Labeled $^{15}NH_4Cl$ and D_2O were purchased from Cambridge Isotope Laboratories. All other chemicals used were of high-quality analytical grade. All experiments were performed at 25 °C. Unless specified, all solutions were made in 10 mM Tris buffer (pH 7.5) containing 100 mM NaCl.

Protein Purification and Isotope Enrichment. cDNA encoding the C2A domain of rat synaptotagmin I (residues 140−267) was kindly provided by T. Sudhof. The cells were induced when A_{600} (absorbance at 600 nm) reached 0.5−0.6 and harvested by centrifugation at 6000 rpm after 4 h. The harvested cells were resuspended, and cell walls were broken by sonication. The cell lysate was centrifuged at 16 000 rpm for 20 min. The supernatant was then incubated with glutathione−Sepharose. For the standard preparations, the resin was extensively washed with PBS until there was no detectable UV absorption in the eluate and cleaved with thrombin (1 NIH unit/mL) at 25 °C for 8 h. The cleaved protein (C2A) was eluted with the PBS buffer. The C2A that was obtained was further purified by gel filtration on a Superdex 75 (Pharmacia) column by FPLC using 10 mM Tris-HCl (pH 7.5, containing 100 mM NaCl) as the eluent. The homogeneity of the protein was assessed using SDS−PAGE. The authenticity of the sample was further verified by electron-spray mass analysis. The concentration of the protein was estimated on the basis of the extinction coefficient value ($\epsilon_{280} = 12\,090\ M^{-1}\ cm^{-1}$) calculated from the amino acid sequence of C2A (*22*).

Preparation of Isotope-Enriched C2A. Uniform ^{15}N labeling was achieved using M9 minimal medium containing $^{15}NH_4Cl$. To achieve maximal expression yields, the composition of the M9 medium was modified by the addition of a mixture of vitamins. The expression host strain *Escherichia coli* BL21 (DE3) pLysS is a vitamin B_1-deficient host, and hence, the medium was supplemented with thiamine (vitamin B_1). The extent of ^{15}N labeling was verified by electron-spray mass analysis.

Isothermal Titration Calorimetry. Binding of Cu^{2+} to C2A was analyzed by measuring the heat change during the titration of Cu^{2+} into a protein solution using a VP-ITC titration microcalorimeter (MicroCal Inc., Northampton, MA). All protein and ligand (Cu^{2+}) solutions were degassed under vacuum and equilibrated at 25 °C prior to titration. The sample cell (1.4 mL) contained 0.1 mM C2A dissolved in 10 mM Tris buffer (pH 7.5) containing 100 mM NaCl. The reference cell contained Milli Q water. Upon equilibration, 2 mM Cu^{2+} was injected in 47 × 6 μL aliquots using the default injection rate. The resulting titration curves were corrected for the protein-free buffer [10 mM Tris (pH 7.5) containing 100 mM NaCl] control and analyzed using the Origin ITC software supplied by MicroCal Inc. The binding constants were estimated from the obtained isotherms using the one-site and sequential binding models.

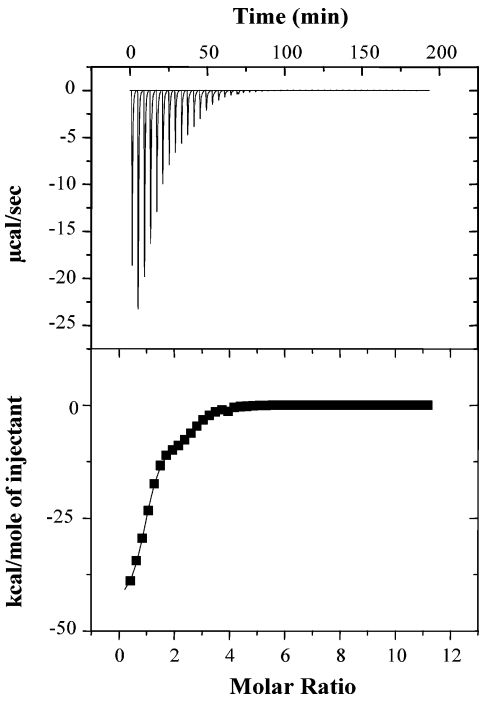

FIGURE 1: Isothermogram representing the binding of Cu^{2+} ions to C2A. The top panel depicts the raw data, and the bottom panel is a best fit of the raw data. The isothermogram fits best to a two-site binding model. C2A binds to Cu^{2+} with a 1:4 stoichiometry. The apparent binding constants [$K_{d(app)}$] of the two Cu^{2+} binding sites are in the low nanomolar (high-affinity site) and high nanomolar (low-affinity site) range. The ΔH_1 and ΔH_2 values are estimated to be -3.6 ± 0.06 and -6.1 ± 0.06 kcal/mol, respectively. Appropriate background corrections were added to account for the heats of dilution and ionization. The concentration of the protein used was 0.1 mM. All experiments were performed at 25 °C.

Absorption Spectroscopy. UV−visible absorption spectra were obtained on a Hitachi U-2910 spectrophotometer using 1 cm path length quartz cuvettes. All measurements were taken after incubation for 2 min (at room temperature) of C2A in appropriate concentrations of Cu^{2+}. The pH was maintained at pH 7.5 by addition of small volumes of 0.1 M NaOH or 0.1 M HCl. The concentration of the protein used in the UV−visible experiments was ~100 μM. Blank corrections were made in all the spectra using protein-free Tris buffer [10 mM Tris (pH 7.5) and 100 mM NaCl] containing an appropriate concentration of Cu^{2+}.

Circular Dichroism. All CD measurements were taken on a Jasco J-720 spectropolarimeter. CD experiments were carried out in Tris buffer (pH 7.5 and 25 °C) using cells with a path length of 1 cm. Stock solutions of Cu^{2+} were prepared by mixing appropriate amounts of $CuCl_2$ in 10 mM Tris buffer (pH 7.5) containing 100 mM NaCl. The pH of the solutions was adjusted to 7.5 by addition of small volumes of 0.1 M NaOH or 0.1 M HCl. CD spectra are an average of at least 10 scans. The concentration of protein used in the CD experiments was ~100 μM.

Size-Exclusion Chromatography. Gel filtration experiments were carried out at 25 °C on a Superdex-75 column using

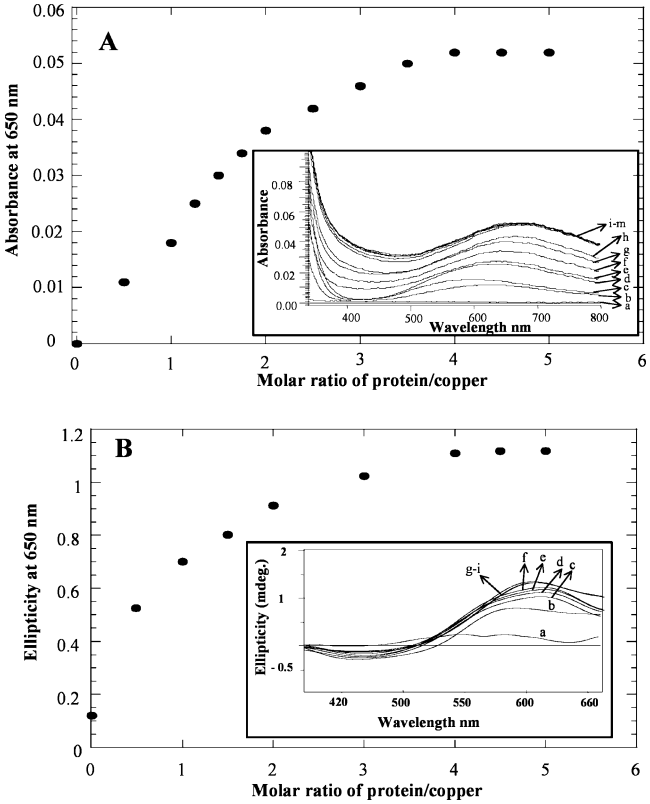

FIGURE 2: (A) Change in absorbance at 650 nm upon addition of an increasing number of equivalents of Cu^{2+} to C2A. The inset shows portions of the absorption spectra of C2A at various concentrations of Cu^{2+}: (a) 0, (b) 50, (c) 100, (d) 125, (e) 150, (f) 175, (g) 200, (h) 250, (i) 300, (j) 350, (k) 400, (l) 450, and (m) 500 μM. The concentration of protein used was 100 μM. Appropriate background corrections were made in all spectra. (B) Change in ellipticity at 650 nm upon addition of Cu^{2+} to C2A. The inset shows portions of the near-UV CD spectra obtained at various concentrations of Cu^{2+}: (a) 0, (b) 50, (c) 100, (d) 150, (e) 200, (f) 250, (g) 300, (h) 400, and (i) 500 μM. The concentration of protein used in these experiments was 100 μM. Necessary background corrections were made in all the spectra. These results show that Cu^{2+} binds to C2A at a ratio of 4:1.

an AKTA FPLC device (Amersham-Pharmacia Biotech). The column was equilibrated with 2 bed volumes of the buffer [10 mM Tris (pH 7.5) containing 100 mM NaCl] and 1 mM $CuCl_2$. The concentration of the protein used in the size-exclusion chromatography experiments was ~200 μM.

Steady State Fluorescence. Fluorescence experiments were performed on a Hitachi F2500 spectrofluorimeter. Appropriate corrections were made for background noise. All fluorescence experiments were performed at 25 °C. For terbium titrations, a stock solution of 50 mM $TbCl_3$ in 10 mM Tris (pH 7.5), containing 100 mM NaCl, was prepared from a standard 1 M $TbCl_3$ solution. Fluorescence spectra of Tb^{3+} were measured on a Hitachi F2500 spectrofluorimeter using a quartz cell with a light path of 10 mm. The excitation wavelength was set at 280 nm, and bandwidths for excitation and emission lights were set at 2.5 and 10 nm, respectively. Terbium titration measurements were taken at a protein concentration of 75 μM.

Proteolytic Digestion Assay. Limited proteolytic digestion experiments on apo-C2A and C2A with Cu^{2+} were carried out at 25 ± 2 °C using trypsin (Sigma Co.). Proteolytic digestions were performed at an enzyme (trypsin) to substrate (C2A) molar ratio of 1:10. The protease activity was stopped after a desired time interval by the addition of the gel loading dye (Bio-Rad) at 80 ± 2 °C. The degree of proteolytic cleavage was measured from the intensity of the ~18 kDa band (on a SDS−PAGE gel) corresponding to the uncleaved protein (C2A) using a densitometer. The intensity of the ~18 kDa band (C2A) not subjected to protease treatment was considered as a control for 100% protection against trypsin cleavage. Control experiments with lysozyme and bovine serum albumin were performed to examine the possible effects of Cu^{2+} ions on trypsin activity.

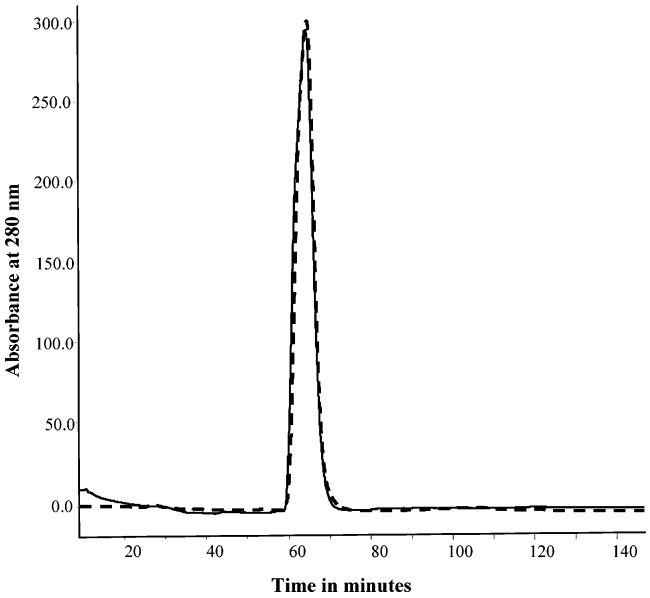

FIGURE 3: Size-exclusion chromatography profile of C2A in the presence (− − −) and absence (—) of Cu^{2+}. The elution of the protein was monitored by 280 nm absorbance. The eluent used was 10 mM Tris-HCl buffer (pH 7.5) containing 100 mM NaCl and 500 μM Cu^{2+}. The concentration of the protein used was 100 μM. All experiments were performed at 25 °C. The elution times of the protein domain (C2A), in the presence and absence of Cu^{2+} ions, are 64 ± 1 and 64 ± 0.5 min, respectively.

NMR Experiments. All NMR experiments were performed on a Bruker Avance 700 MHz NMR spectrometer equipped with a cryoprobe at 25 °C. ^{15}N decoupling during acquisition was accomplished using the globally optimized altering-phase rectangular pulse sequence; 2048 complex data points were collected in the ^{15}N dimension. $^{1}H-^{15}N$ HSQC spectra were recorded at 64 scans at all concentrations of Cu^{2+}. The concentration of the protein sample that was used was 0.1 mM in 90% H_2O and 10% D_2O [10 mM Tris (pH 7.5) containing 100 mM NaCl]. Spectral intensities were corrected for dilution effects. All the spectra were processed on a Windows workstation using Xwin-NMR and Sparky (*52*).

RESULTS AND DISCUSSION

The C2A domain of p40Syt is an 18 kDa all-β-sheet protein devoid of disulfide bonds (hereafter termed C2A) (*17*, *18*). The secondary structural elements in C2A include eight β-strands arranged into a β-sandwich architecture. C2A is a calcium binding domain and binds to 3 equiv of calcium (*17*−*19*).

C2A Has a High Affinity for Cu^{2+}. Isothermal titration calorimetry (ITC) is an important tool for studying both thermodynamic and kinetic properties of biological macromolecules by virtue of its general applicability and high level

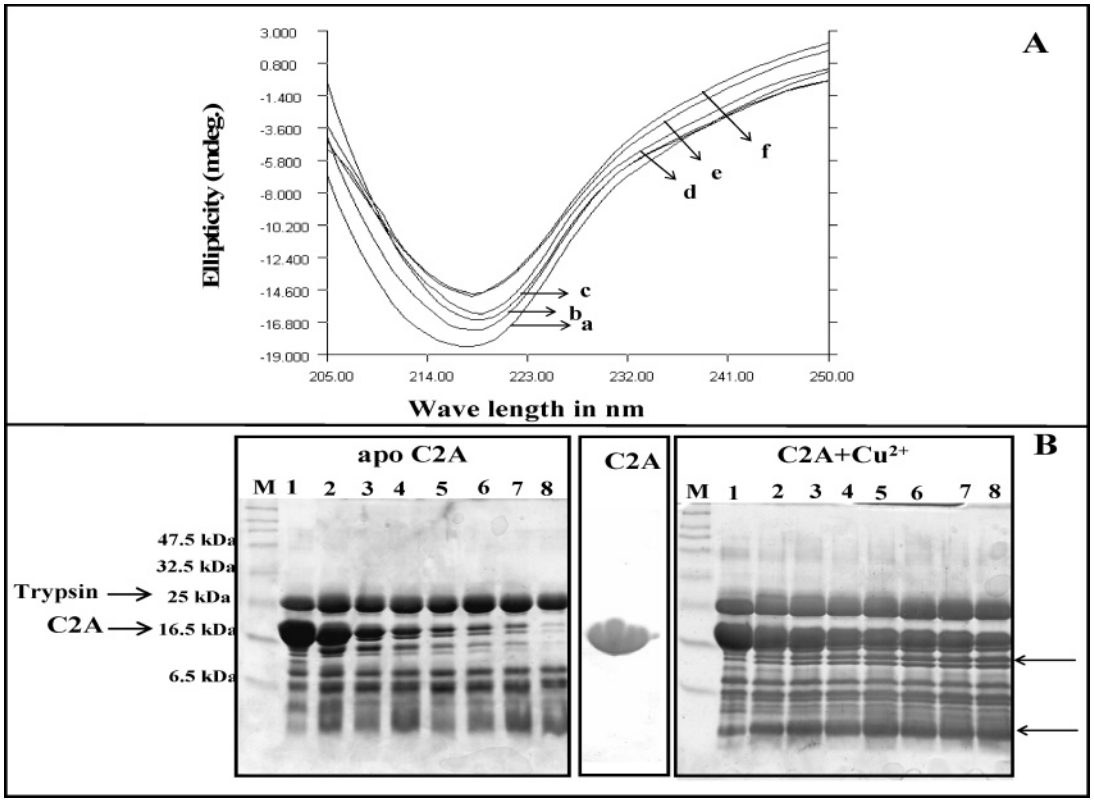

FIGURE 4: (A) Far-UV CD spectra of C2A in the presence of various concentrations of Cu^{2+}: (a) 0, (b) 100, (c) 200, (d) 300, (e) 400, and (f) 500 μM. The concentration of protein used was 100 μM. All spectra are an average of 10 scans. All spectra were corrected for background noise. (B) SDS−PAGE analysis of the trypsin digestion products of C2A in the absence (apo form) and presence of Cu^{2+}. The lane marked C2A represents the protein domain band in the absence of typsin. Lane M shows the molecular weight marker. Lanes 1−8 contained the trypsin digestion products of C2A at various time periods of incubation of C2A with trypsin in the absence (apo form) and presence of Cu^{2+}: lane 1, 2 min; lane 2, 5 min; lane 3, 10 min; lane 4, 15 min; lane 5, 20 min; lane 6, 25 min; lane 7, 30 min; and lane 8, 40 min. The ratio of C2A to trypsin was 1:10. The arrows indicate the additional digestion products of C2A in the presence of Cu^{2+}. These products are not observed when C2A alone is treated with trypsin. The gel was stained with Coomassie blue. The data suggest that the protein undergoes a subtle conformational change in the presence of Cu^{2+}.

of precision (*21*, *23*). ITC experiments have been successfully used to investigate binding affinities of proteins for ligands and metal ions (*23*). The thermodynamics of binding of Cu^{2+} ions to C2A has been investigated using ITC. The binding isotherm representing the binding of Cu^{2+} ions to C2A is hyperbolic and proceeds with the evolution of heat (Figure 1). The hyperbolic binding isotherm does not permit the accurate estimation of the binding constant and other thermodynamic parameters characterizing the interaction of C2A with Cu^{2+}. The value of the apparent change in enthalpy (ΔH_{app}) of the reaction is negative, suggesting that charge interactions play a dominant role in the binding of Cu^{2+} ions to C2A. The Cu^{2+}−C2A titration curve saturates at a Cu^{2+} to C2A binding ratio of 4:1 (Figure 1). Least-squares fitting of the Cu^{2+}−C2A binding isotherm yields an "*n*" value of ~2, indicating that there are two types of Cu^{2+} binding sites in C2A. The apparent binding constant [$K_{d(app)}$] values of the two copper binding sites are in the nanomolar range. The $K_{d(app)}$ of the high-affinity binding site is at least 15 times lower than that of the low-affinity binding site. Previously, C2A has been only shown to bind to Ca^{2+} (*15*, *16*). This is the first time the high Cu^{2+} binding affinity of C2A has been demonstrated. Interestingly, the binding affinity of C2A for Cu^{2+} far exceeds its affinity for Ca^{2+} (*15*−*17*, *24*; to be discussed later).

Stoichiometry of Binding of Cu^{2+} to C2A. Although ITC experiments provide a reliable estimate of the binding stoichiometry, these estimates derived from ITC data can be skewed due to the contributions arising from heats of ionization and dilution (*25*). Therefore, we examined the stoichiometry of binding of Cu^{2+} and C2A using visible spectrophotometry and circular dichroism spectroscopy. Metal ions upon binding to macromolecules such as proteins exhibit prominent peaks in the visible region of the absorption spectra (*26*). These absorption bands are commonly called the Soret bands (*26*). The absorption spectrum of C2A in the presence of Cu^{2+} shows a Soret type of absorption band at 650 nm (Figure 2A, inset). The intensity of the Soret-type band increases with an increasing number of equivalents of Cu^{2+} (Figure 2A). Interestingly, there is a gradual red shift in the wavelength maximum of the Soret-type band with an increase in the concentration of Cu^{2+} suggestive of minor conformational changes induced in the protein by Cu^{2+}. The spectral changes are complete upon addition of 4 equiv of Cu^{2+}, implying that one molecule of C2A binds to four Cu^{2+} ions (Figure 2A).

The near-UV circular dichroism (CD) spectrum of apo C2A shows no perceivable signal beyond 400 nm. Addition of Cu^{2+} results in a prominent CD band centered at 650 nm (Figure 2B, inset). The intensity of the CD band at 650 nm progressively increases with an increase in the concentration of Cu^{2+} (Figure 2B). In addition, a prominent 50 nm (from 600 to 650 nm) red shift could be discerned when the number of equivalents of Cu^{2+} added was increased from 0 to 4

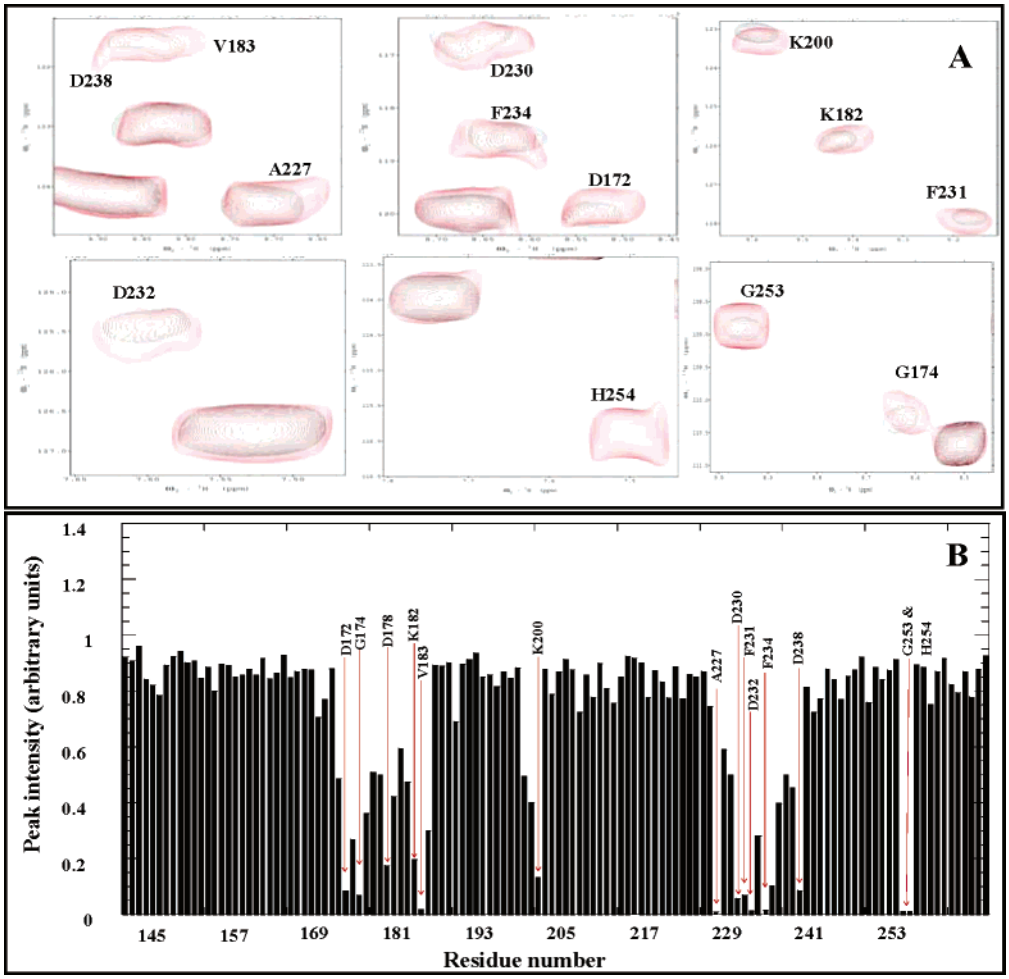

FIGURE 5: (A) Portions of $^{1}H-^{15}N$ HSQC spectra of C2A obtained in the absence (red) and presence (black) of Cu^{2+}. The significant decrease in the cross-peak intensity observed in the presence of Cu^{2+} indicates that these residues are in the vicinity of the Cu^{2+} binding site(s). (B) Plot showing the cross-peak intensity of residues in the $^{1}H-^{15}N$ HSQC spectrum of C2A in the presence of Cu^{2+}. The cross-peaks which exhibit a significant decrease in intensity represent the Cu^{2+} binding sites in C2A. The $^{1}H-^{15}N$ HSQC spectrum in the presence of Cu^{2+} was obtained at a protein to metal ratio of 1:4.

(Figure 2B, inset). The significant red shift in the near-UV CD band can be ascribed to conformational changes induced in C2A by Cu^{2+}. The changes in the CD band are complete after addition of 4 equiv of Cu^{2+} (Figure 2B). The results of the absorption spectroscopy and CD spectroscopy completely corroborate each other and clearly show that the C2A binds to Cu^{2+} at a ratio of 1:4. In addition, these results also indicate that C2A undergoes a small conformational change upon binding to Cu^{2+}.

The Molecular State of C2A Does Not Change upon Binding of Cu^{2+}. Proteins are known to undergo dimerization and/or oligomerization upon binding to Cu^{2+} (*27*). In this context, it is important to investigate if Cu^{2+} changes the molecular state of C2A. Size-exclusion chromatography is a useful technique for monitoring the molecular association and dissociation of proteins upon metal−ligand binding (*28*). Under the experimental conditions that were used, free C2A elutes with an elution time of 64 ± 1 min (Figure 3). The elution time of the protein does not change significantly even when eluted in the presence of an excess of Cu^{2+} ions (>10 equiv). These results unambiguously suggest that C2A remains in its monomeric state upon binding to Cu^{2+}.

C2A Undergoes Subtle Conformational Change(s) upon Binding to Cu^{2+}. We monitored possible conformational changes in C2A induced by Cu^{2+} using far-UV CD spectroscopy. The far-UV CD spectrum of C2A shows an intense negative ellipticity band centered at around 218 nm, suggesting that the protein domain is an all-β-sheet with no helical segments (Figure 4A). This observation is consistent with the three-dimensional structures of C2A, which show that the protein contains eight β-strands arranged into a β-sandwich architecture (*29*, *30*). Addition of incremental amounts of Cu^{2+} shows a small (~10%) but significant decrease in the intensity of the CD band at 218 nm (Figure 4A). These results indicate the C2A undergoes mild conformational change(s) upon binding to Cu^{2+}, resulting in a decrease in the average β-sheet content in the protein. An increase in Cu^{2+} concentration beyond a protein to metal ratio of 1:4 causes no or very insignificant change in the 218 nm ellipticity (Figure 4A). Limited proteolytic digestion has been successfully employed to investigate the conformational flexibility of proteins (*31*). The basic premise underlying this technique is that the proteolysis event is governed by the stereochemistry and accessibility of the protein substrate as well as the specificity of the proteolytic enzyme. Hence, even subtle conformational changes in the protein can be successfully detected using the limited proteolytic digestion technique. C2A contains many lysine and arginine residues in its sequence (*32*). As the cleavage sites for trypsin correspond to the carbonyl groups of lysine

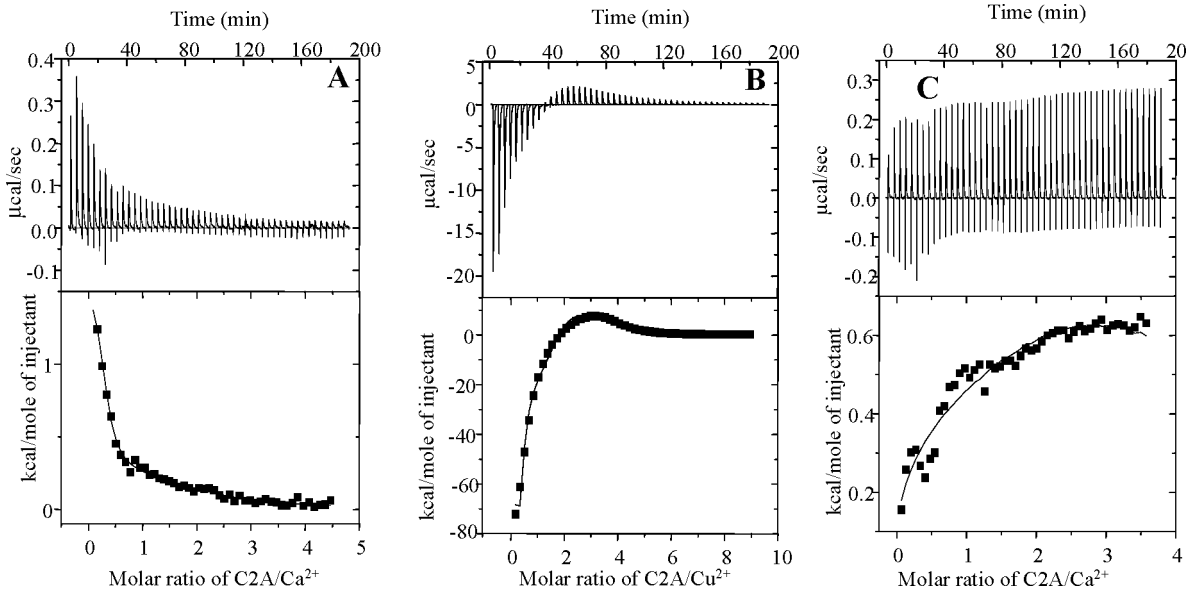

FIGURE 6: Isothermogram representing the titration of (A) C2A with Ca^{2+}, (B) C2A [in the presence of saturating amounts (500 μM) of Ca^{2+}] with Cu^{2+}, and (C) C2A [in the presence of a saturating concentration (500 μM) of Cu^{2+}] with Ca^{2+}. The stoichiometry of C2A to Ca^{2+} binding is estimated to be 1:3. The binding of Cu^{2+} does not appear to be significantly affected in the presence of saturating amounts of Ca^{2+}. In the presence of saturating amounts of Ca^{2+}, 4 equiv of Cu^{2+} binds to C2A (B). Interestingly, only 1 equiv of Ca^{2+} appears to bind to C2A in the presence of a saturating concentration (500 μM) of Cu^{2+} (C). These results suggest that Cu^{2+} ions and Ca^{2+} ions share common binding sites in C2A.

and arginine residues, trypsin is an apt choice for monitoring the conformational differences that possibly exist between apo-C2A and the Cu^{2+}-bound form of C2A. Undigested C2A yields a band on SDS−PAGE that corresponds to a molecular mass of ~18 kDa (Figure 4B). The intensity of this band (upon Coomassie blue staining) is used as an indicator of the degree of susceptibility of C2A to trypsin action. It could be observed that the intensity of the ~18 kDa band corresponding to the intact C2A decreases with the increase in the time of incubation with trypsin (Figure 4B). The apo form of C2A is completely digested after incubation with the enzyme for 20 min. In marked contrast, in the presence of Cu^{2+}, more than 50% of the ~18 kDa band remains undigested even after digestion for 60 min, suggesting that the conformational flexibility of C2A decreases significantly upon binding to Cu^{2+}. The products of trypsin digestion of C2A in the presence and absence of the metal are distinctly different (Figure 4B). The difference(s) in the enzyme digestion pattern clearly indicates that the metal (Cu^{2+}) induces a subtle conformational change that alters the degree of exposure of the enzyme cleavage sites in the protein (C2A). It may be argued that the difference(s) observed in the digestion pattern could be due to the altered cleavage specificity of the enzyme (trypsin) in the presence of Cu^{2+}. This contention could be discounted because control trypsin cleavage experiments using lysozyme and bovine serum albumin in the presence and absence of Cu^{2+} showed that the metal does not alter the cleavage specificity of the enzyme (data not shown).

Identification of Cu^{2+} Binding Sites in C2A. The $^1H-^{15}N$ HSQC spectrum is a fingerprint of the backbone conformation of a protein (*33*). Each $^1H-^{15}N$ cross-peak represents the microenvironment of an amino acid in the protein. The disappearance or chemical shift perturbation of cross-peaks in the $^1H-^{15}N$ HSQC spectrum upon addition of metal or ligand provides useful information about the metal or ligand interaction sites in the protein.

Cu^{2+} is paramagnetic, and therefore, resonances of residues (in the $^1H-^{15}N$ HSQC spectra) in the immediate vicinity of Cu^{2+} binding sites in the protein are broadened sometimes beyond detection (*34*). The extent of paramagnetically induced line broadening depends on the electronic relaxation time of the metal center (*34*). In this context, the binding of Cu^{2+} binding sites in C2A was identified by the diminishing intensities of selected cross-peaks in the $^1H-^{15}N$ HSQC spectra. The $^1H-^{15}N$ HSQC spectrum of apo-C2A is well-dispersed, and all the cross-peaks in the $^1H-^{15}N$ HSQC spectrum of C2A have been assigned (*29*, *30*). This aspect allowed us to identify residues in C2A that bind to Cu^{2+}. The intensities of selected $^1H-^{15}N$ HSQC cross-peaks are observed to decrease upon increased additions of Cu^{2+}. The residues that undergo a drastic decrease in intensity are located in the three loop (loops 1−3) structures that project out of the β-sandwich structure of C2A (Figure 5A,B). These residues include Asp172, Gly174, Asp178, Lys182, and Val183 (in loop 1), Lys200 (in loop 2), and Ala227, Asp230, Phe231, Asp232, Phe243, and Asp238 (in loop 3). In addition, the cross-peaks representing two residues (Gly253 and His254) located in the loop linking β-strands 7 and 8 also tend to disappear completely in the presence of Cu^{2+} (Figure 5A,B). These results indicate that the Cu^{2+} binding sites in C2A are distributed in loops 1−3 and a remote site in the unstructured loop located between β-strands 7 and 8. $^1H-^{15}N$ HSQC data analyzed in conjunction with the ITC data suggest that the three Cu^{2+} ions bind to the high-affinity binding site located in the three loops at the apex of the C2A structure. One Cu^{2+} ion appears to bind to the low-affinity site located in the loop between β-strands 7 and 8. Interestingly, the Cu^{2+} binding residues that are in loops 1−3 have also been shown to bind to calcium (*16*, *29*, *30*; to be discussed later).

Cu^{2+} and Ca^{2+} Ions Share Common Binding Sites in C2A. The role(s) of the C2A and C2B domains of Syt1 in calcium-triggered neurosecretion is well-established (*35*). Binding of

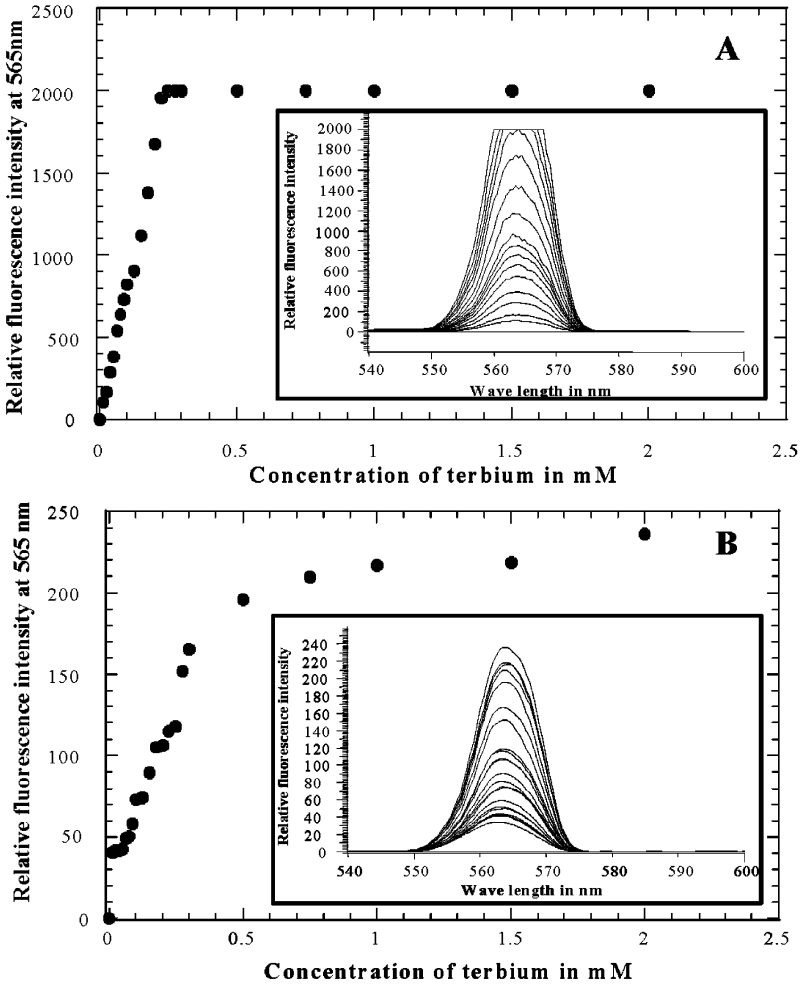

FIGURE 7: Terbium binding to C2A. (A) Titration of C2A with Tb^{3+} (0−2 mM) monitored by fluorescence emission at 565 nm. The inset shows a portion of the emission spectra of Tb^{3+} in the presence of C2A. (B) Increase in Tb^{3+} fluorescence intensity (at 565 nm) in the presence of C2A and a saturating concentration of Cu^{2+} (500 μM). The inset shows emission spectra at increasing concentrations of Tb^{3+}. It could be discerned that the maximum relative fluorescence intensity (at 565 nm) value in the presence of saturating concentrations of Cu^{2+} is ~10% of that obtained in the absence of Cu^{2+}. These results suggest that Cu^{2+} competes for the Ca^{2+} binding sites in C2A. The concentration of C2A used was 75 μM. The buffer used was 10 mM Tris-HCl (pH 7.5) containing 100 mM NaCl.

Ca^{2+} to C2A enhances the association of Syt1 with several other proteins involved in neurotransmission, including syntaxin 1A (*36*). In addition, binding of Ca^{2+} to C2A promotes its insertion into membranes via interaction with acidic phospholipids (*37*). The three-dimensional structures of C2A of Syt1 are available (*30*, *35*). Ca^{2+} binds exclusively to the loops (loops 1−3) located at the apex of the β-sandwich structure of C2A. These loops coordinate three Ca^{2+} ions primarily via multidentate aspartic acid residues (*38*). Binding of calcium does not induce any significant conformational change in C2A.

We used ITC, terbium-based fluorescence energy transfer, and NMR spectroscopy to assess the possible competition between Ca^{2+} and Cu^{2+} for binding to C2A. The isothermogram representing binding of Ca^{2+} to C2A is endothermic and proceeds with absorption of heat (Figure 6A). Least-squares fitting of the titration curve shows that 3 equiv of Ca^{2+} binds to C2A with similar binding affinities (in the millimolar range). These results agree well with the available solution structure of the C2A−Ca^{2+} complex (*30*, *35*). The isothermogram representing the titration of C2A (saturated with 500 μM Ca^{2+}) with Cu^{2+} is hyperbolic and proceeds with the evolution of heat (Figure 6B). The protein to Cu^{2+} binding ratio is estimated to be 1:4. Interestingly, the apparent binding constant(s) of the high-affinity copper binding site in the presence of saturating amounts of Ca^{2+} is in the low nanomolar range. The apparent binding constant values at the high-affinity site for the C2A−Cu^{2+} interaction is in the same range (low nanomolar range), when the titration is performed in the absence of Ca^{2+}. These results clearly demonstrate that Cu^{2+} ions can bind to C2A even in the presence of calcium. It appears that at least some of the metal binding sites on C2A are common to both Ca^{2+} and Cu^{2+} ions. ITC experiments were performed to examine if Ca^{2+} ions can competitively displace Cu^{2+} ions bound to C2A. The isothermogram representing the C2A−Ca^{2+} interaction [in the presence of saturating concentrations (500 μM) of Cu^{2+} ions] shows that the binding of the protein to Ca^{2+} under these conditions is weak (Figure 6C). The interaction is exothermic and proceeds with the evolution of heat. The titration curve saturates at a protein to Ca^{2+} ratio of 1:1, indicating that in the presence of Cu^{2+} only 1 equiv of Ca^{2+} binds to C2A. Results of ITC experiments clearly suggest that Cu^{2+} ions can reversibly displace Ca^{2+} ions bound to C2A, but only one of the four Cu^{2+} ions bound to the protein can be replaced by Ca^{2+} ions.

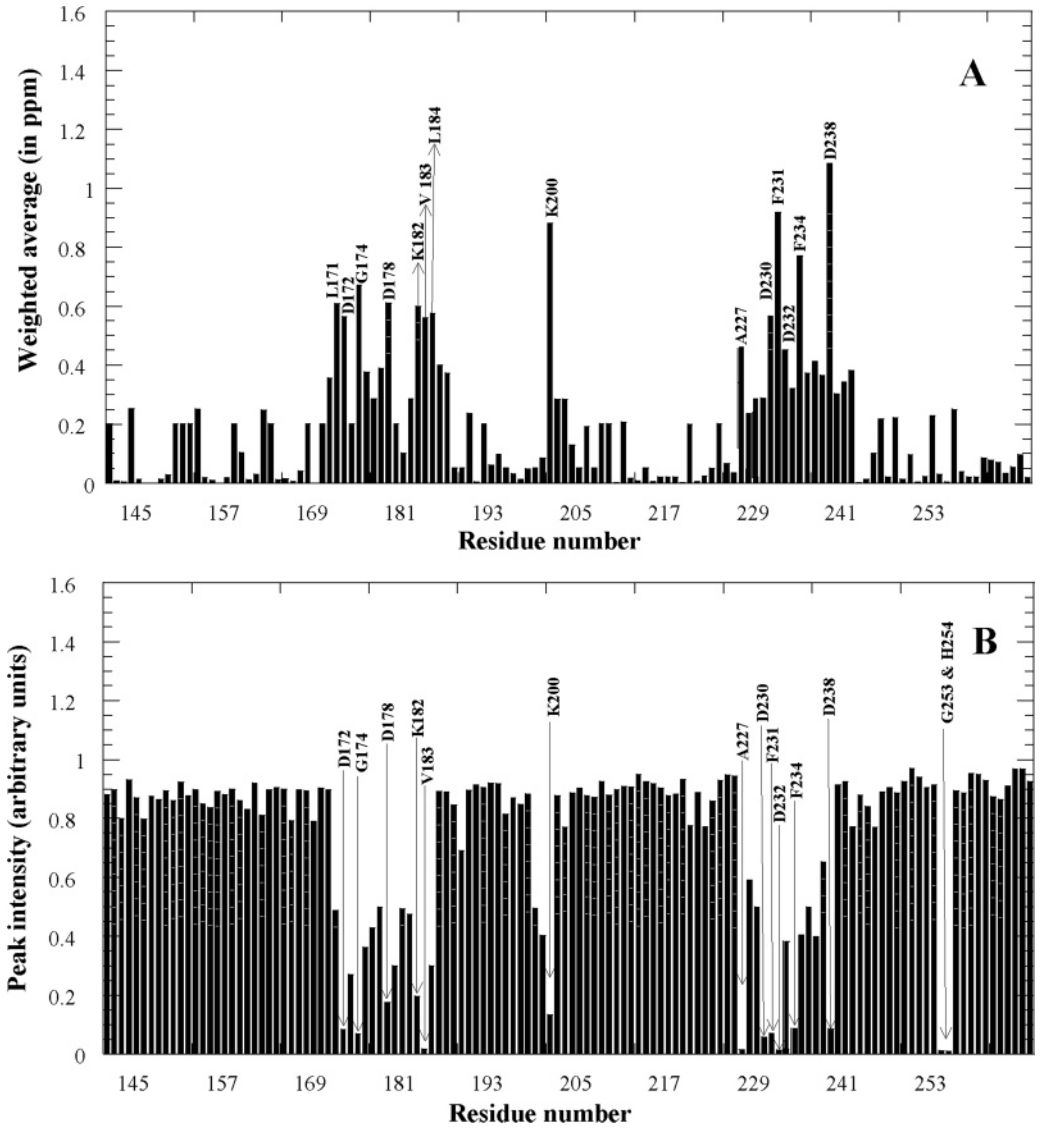

FIGURE 8: (A) $^{1}H-^{15}N$ chemical shift perturbation of residues of C2A in the presence of Ca^{2+} (1 mM). The amino acid residues in C2A that exhibited significant chemical shift perturbation and are involved in Ca^{2+} binding are indicated by the single-letter code. (B) Cross-peak intensity of residues in the $^{1}H-^{15}N$ HSQC spectrum of C2A obtained in the presence of 400 μM Cu^{2+} and saturating amounts of Ca^{2+} (1 mM). The cross-peaks that exhibit a significant decrease in their intensities represent the Cu^{2+} binding sites in C2A. Interestingly, comparison of data shown in panels A and B reveals that Cu^{2+} and Ca^{2+} share common binding sites in C2A. Gly253 and His254 represent an additional Cu^{2+} binding site in C2A (B). The concentration of protein used was 100 μM. The buffer solutions were prepared in 90% H_2O and 10% D_2O containing 10 mM Tris-HCl (pH 7.5) and 100 mM NaCl. $^{1}H-^{15}N$ HSQC experiments were conducted at 25 °C.

The competition between Ca^{2+} and Cu^{2+} ions for binding to C2A was further probed using the calcium binding probe, terbium, by fluorescence energy transfer (FRET). Terbium (Tb^{3+}) is known to bind to calcium binding sites and induce luminescence at 565 nm via energy transfer from the tryptophan residues (*39*). Figure 7 shows that Tb^{3+} binds to C2A and induces luminescence at 565 nm. The tryptophan fluorescence intensity at 340 nm shows a steady decrease with the increase in the Tb^{3+} concentration. The decrease in tryptophan fluorescence intensity is compounded by a concomitant increase in the Tb^{3+} fluorescence at 565 nm, suggesting an energy transfer from tryptophan residues in the protein to the Tb^{3+} ions bound to C2A (Figure 7A). The relative fluorescence intensity (at 565 nm) value reaches a maximum value of ~2000 at a C2A to Tb^{3+} ratio of 1:3. The C2A$-Tb^{3+}$ titration curve saturates beyond a protein to Tb^{3+} ratio of 1:3, indicating that three Tb^{3+} ions bind to one molecule of C2A. The binding stoichiometry data derived from Tb^{3+} binding experiments are consistent with a 1:3 C2A to Ca^{2+} binding ratio reported by Rizo and co-workers (*30*, *35*).

Tb^{3+} binding experiments were performed by titrating C2A with Tb^{3+} in the presence of saturating concentrations of Cu^{2+} (~500 μM). Increasing additions of Tb^{3+} to the protein result in an increase in the Tb^{3+} fluorescence intensity at 565 nm (Figure 7B). The Tb^{3+} fluorescence intensity reaches a plateau when the Tb^{3+} concentration reaches 0.75 mM. A further increase in Tb^{3+} concentration does not significantly increase the fluorescence intensity at 565 nm (Figure 7B). In the presence of saturating concentrations of Cu^{2+}, the maximum relative fluorescence intensity at 565 nm is only ~10% of the value obtained in the absence of Cu^{2+} ions (Figure 7A,B). These results suggest that while Cu^{2+} ions can completely force out Ca^{2+} ions bound to C2A, the reverse is not true. The small marginal increase in the Tb^{3+} fluorescence observed in the presence of saturating concen-

trations of Cu^{2+} implies that Ca^{2+} ions can only partially replace the Cu^{2+} ions bound to the protein. Therefore, results of the Tb^{3+} binding experiments are in good agreement with the ITC data that unambiguously suggest that Ca^{2+} ions cannot competitively displace the Cu^{2+} ions bound to the protein. It is interesting to understand why Ca^{2+} ions cannot reversibly compete with Cu^{2+} ions to bind to C2A even though the two metal ions appear to share common binding sites on the protein. Although at present we do not have a concrete explanation for the observed anomaly, we believe that subtle conformational changes induced in C2A by Cu^{2+} ions appear to render the metal binding sites inaccessible to Ca^{2+} binding. On the other hand, binding of Ca^{2+} to C2A occurs without any significant conformational change in the protein. This aspect (compounded by the higher binding affinity of C2A for Cu^{2+} ions) facilitates the competitive displacement of Ca^{2+} ions bound to the protein by Cu^{2+} ions.

The competition between the metal ions (Ca^{2+} and Cu^{2+}) for binding to C2A can be unambiguously monitored by two-dimensional $^{1}H-^{15}N$ HSQC spectra. The C2A domain is known to bind to 3 equiv of Ca^{2+} (*30*, *35*). As mentioned earlier, binding of Ca^{2+} does not induce conformational changes in C2A. Ca^{2+} ions have been proposed to stabilize the protein by binding to the negatively charged aspartic acid residues located on the top of the β-sandwich structure of C2A (*30*, *35*).

Several cross-peaks corresponding to residues Leu171, Asp172, Gly174, Asp178, Lys182, Val183, Leu184, Asp230, Phe231, Asp232, Phe234, and Asp238 show prominent chemical shift perturbation in the presence of Ca^{2+} (Figure 8A). These residues are located in loops 1−3 and constitute the calcium binding sites. If Cu^{2+} ions share binding sites with Ca^{2+} and displace it, then one would expect the intensity of the cross-peaks of residues involved in Ca^{2+} binding to be diminished due to the paramagnetic line broadening effects of Cu^{2+}. The $^{1}H-^{15}N$ HSQC spectrum of C2A (saturated with Ca^{2+}), obtained at a protein to Cu^{2+} ratio of 1:4, shows that the cross-peaks of residues involved in Ca^{2+} binding almost completely disappeared (Figure 8B). In addition to these residues, two other cross-peaks representing Gly253 and His254 also show a significant decrease in intensity upon titration with Cu^{2+} ions (Figure 8B). These two residues are located at sites remote from the loop structure that are involved in the binding of 3 equiv of Cu^{2+} or Ca^{2+} ions (Figure 9). In summary, these results suggest that residues that bind to Ca^{2+} in C2A are also involved in Cu^{2+} binding. In addition, His254 and Gly253 constitute a unique Cu^{2+} binding site in C2A (Figure 9). His254 and Gly253 are not involved in Ca^{2+} binding.

Possible Physiological Significance of Binding of Cu^{2+} to C2A. It is interesting to find that C2A binds to Cu^{2+} with extraordinarily high affinity (in the nanomolar range). There are many examples of calcium binding proteins (like C2A) binding to transition metals such as copper and zinc. Several members of the S100 family have been shown to bind with both Cu^{2+} and Zn^{2+} (*40*−*42*). S100B is relatively abundant in the brain and binds to both zinc and copper (*43*). Interestingly, S100B is believed to play an important role in copper hemeostasis as well as in prevention of copper-induced oxidative damage in brain (*44*). Although the exact biological function of these transition metals in S100 proteins is not fully understood, these divalent cations are proposed

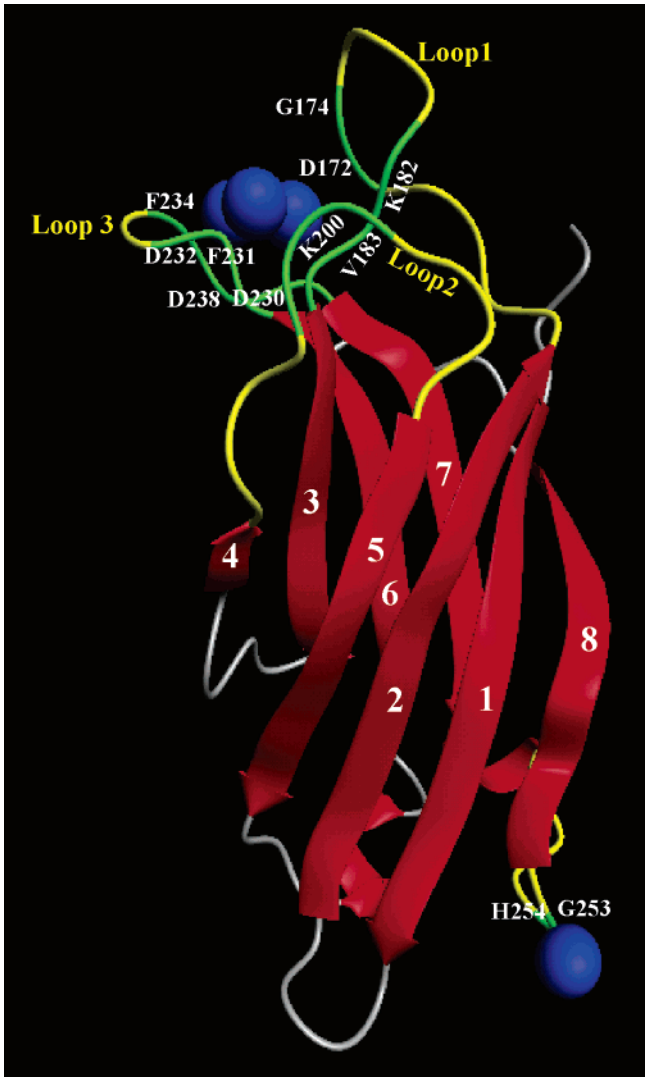

FIGURE 9: MOLMOL (*51*) representation of the backbone folding of C2A. Four Cu^{2+} ions are shown to bind to C2A. Three of the Cu^{2+} ions bind to the loops located at the top portion of the C2A structure. One Cu^{2+} ion appears to bind to Gly253 and His254 located in the loop between β-strands 7 and 8. The β-strands in the C2A domain are numbered in Arabic numerals.

to play a regulatory role by modulating the affinity for various S100 proteins for Ca^{2+} and protein targets (*43*). For example, once Zn^{2+} binds, the binding affinity of S100B for both Ca^{2+} ions and a peptide derived from the protein CapZ (TRTK) is reported to increase by 10- and 5-fold, respectively (*45*). Similarly, S100A12 binds to Zn^{2+} with a relatively high affinity ($\sim$100 μM) compared to those of other S100 proteins, and Zn^{2+} binding causes a large ($\sim$1500-fold) increase in its affinity for Ca^{2+} (*46*). Without exception, binding of Zn^{2+} to proteins belonging to the S100 family involves a major conformational change (*46*). The change in conformation is believed to contribute to the increased binding affinity of S100 members for Ca^{2+} targeting proteins (*45*, *46*). In the context of the available literature, it will be interesting to understand the physiological significance of the high binding affinity of the C2A domain for Cu^{2+}.

As mentioned previously, FGF-1 is a potent mitogen that lacks the classical signal peptide at its N-terminal end (*10*, *11*). Maciag and co-workers demonstrated that under heat stress, FGF-1 is released into the extracellular medium as a multiprotein complex comprising the homodimer of FGF-1

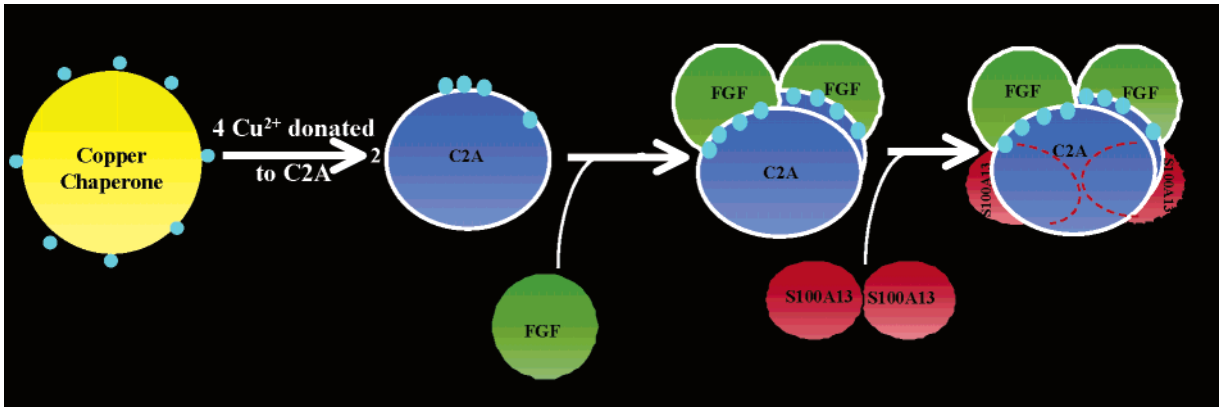

FIGURE 10: Cartoon depicting the possible structural events that occur in the formation of the multiprotein release complex. The first step in the process appears to be the donation of the Cu^{2+} ions (cyan) from a cellular copper storage protein (yellow) to the C2A domain of Syt1 (blue). Each molecule of C2A appears to bind to 4 equiv of Cu^{2+} with very high affinity (in the nanomolar range). Two molecules of FGF-1 (green) appear to bind to the C2A domain at the Cu^{2+} binding site(s). FGF-1 possibly binds to the C2A domain in its monomeric state with the thiol group of Cys30 located close to the copper binding site in C2A. In the third step, the S100A13 dimer (red) appears to bind to the C2A−FGF complex. Dimerization of FGF-1 induced (due to the oxidation of the thiol group of Cys30) by Cu^{2+} appears to occur after the formation of the C2A−FGF-1−S100A13 ternary complex. The dimer alone has low solubility in aqueous solutions, and it appears that C2A and S100A13 together prevent the aggregation of the FGF-1 homodimer.

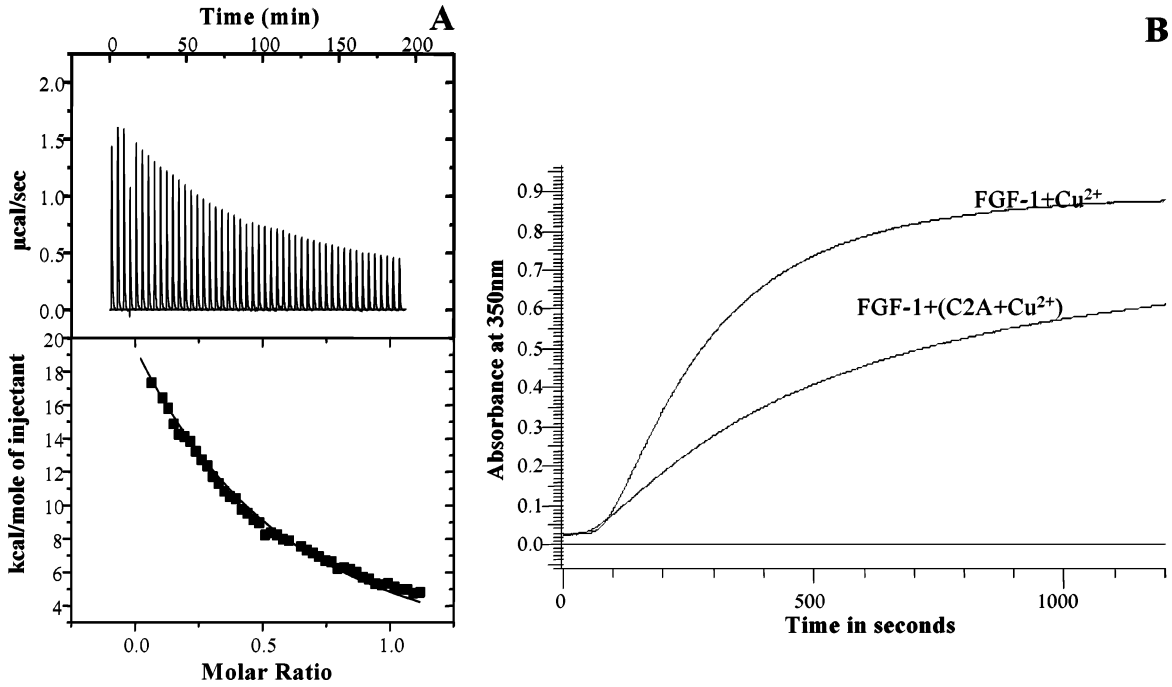

FIGURE 11: (A) Isothermogram showing the binding of C2A with FGF-1. The binding constant [$K_{d(app)}$] characterizing the C2A−FGF-1 interaction is 1.2 μM. The stoichimetry of binding between C2A and FGF is 1:1. The concentrations of C2A and FGF-1 used in the ITC experiments are 1 and 0.1 mM, respectively. The top panel shows the raw titration data, and the bottom panel represents the best fit curve of the raw data. (B) Time-dependent changes in the absorption (scattering) at 350 nm. The concentrations of C2A, FGF-1, and Cu^{2+} used were 0.2, 0.02, and 0.01 mM, respectively. Cu^{2+}-induced oxidation of the thiol group of Cys30 results in the formation of the FGF-1 homodimer. The homodimer has a strong tendency to aggregate in aqueous solution as indicated by the time-dependent increase in the scattering intensity at 350 nm. Interestingly, the C2A domain appears to decrease the extent of aggregation of the FGF-1 homodimer.

and S100A13 and Syt1 (*11*−*14*). The formation of the homodimer of FGF-1 is triggered by Cu^{2+}-induced oxidation of a specific cysteine residue (Cys30) in FGF-1. However, very little is known about the source of Cu^{2+} required for the formation of the homodimer of FGF-1. Identification of the source of Cu^{2+} is important because even traces of Cu^{2+} are toxic to the cells because it leads to the generation of hydroxyl radical and to oxidation damage (*47*).

There is virtually no free copper in cytoplasm, and delivery of copper to vital enzymes occurs via a group of specific metal ion chaperones; e.g., Atx1 delivers Cu^{2+} to Menkes protein, Cox17 to cytochrome *c* oxidase, and Lys7 to superoxide dismutase 1 (*48*−*50*). In general, Cu^{2+} chaperones have moderate affinity for Cu^{2+} [$K_{d(app)}$ in the micromolar range]. This aspect energetically favors the routing of Cu^{2+} to other target Cu^{2+} proteins that exhibit much higher affinity for the metal ion (K_d in the nano- to picomolar range) (*50*). In this background, it is reasonable to assume that the high Cu^{2+} binding affinity of the C2A domain of Syt1 helps it to act like a receptor for receiving Cu^{2+} ions from one of the Cu^{2+} chaperones in the cell (Figure 10). It appears that the Cu^{2+} required in the oxidation of Cys30 for the formation of the FGF-1 homodimer is supplied by the C2A domain of Syt1. FGF-1 possibly binds to the C2A domain as a

monomer, and formation of the FGF-1 dimer is possibly induced on the surface of the C2A domain (Figure 10). This notion is supported by several lines of evidence. (1) Preliminary ITC experiments show that the C2A domain directly interacts with FGF-1 even in the absence of Cu^{2+} with moderate binding affinity [$K_{d(app)}$ in the ~1.2 μM range, Figure 11A]. (2) FGF-1 in the presence of Cu^{2+} instantaneously aggregates due to the coalescence of the homodimer that is formed. However, the aggregation of FGF-1 is significantly decreased in the presence of C2A (Figure 11B). At present, we cannot rule out the possibility of S100A13 acting in concert with C2A to promote the dimerization of FGF-1, because S100A13 like many other S100 family proteins is also known to bind to Cu^{2+} with a relatively low (K_d in the micromolar range) affinity. Irrespective of the involvement of S100A13 in the formation of the FGF-1 homodimer, C2A appears to be the predominant Cu^{2+} donor required for the dimerization reaction.

The functional role(s) of Syt1 appears to be dependent on the type of metal ion it binds. Once Ca^{2+} ions binds, Syt-1 functions as a membrane trafficking protein regulating exocytosis. However, when bound to Cu^{2+}, Syt1 is possibly channeled toward the formation of the multiprotein FGF-1 release complex. It is not clear how the switch from the Ca^{2+}-bound state to the Cu^{2+}-bound state is regulated. It appears that prevention of the formation of the Cu^{2+}-bound state of C2A is an effective strategy for specifically inhibiting the FGF-1-induced pathogenesis.

ACKNOWLEDGMENT

We thank Prof. Thomas Sudhof for kindly providing the C2A clone. We thank the late Prof. Tom Maciag for introducing us to research on the nonclassical release of FGF.

REFERENCES

1. Schlessinger, J. (2004) Common and distinct elements in cellular signaling via EGF and FGF receptors, *Science 306*, 1506−1507.
2. Arunkumar, A. I., Srisailam, S., Kumar, T. K. S., Kathir, K. M., Chi, Y. H., Wang, H. M., Chang, G. G., and Yu, C. (2002) Structure and stability of an acidic fibroblast growth factor from *Notophthalmus viridescens*, *J. Biol. Chem. 277*, 46424−46432.
3. Chi, Y. H., Kumar, T. K., Kathir, K. M., Lin, D. H., Zhu, G., Chiu, I. M., and Yu, C. (2002) Investigation of the structural stability of the human acidic fibroblast growth factor by hydrogen−deuterium exchange, *Biochemistry 41*, 15350−15359.
4. Yu, K., Yu, J., Liu, Z., Sosic, D., Shao, J., Olson, E. N., Towler, D. A., and Ornitz, D. M. (2003) Conditional inactivation of FGF receptor 2 reveals an essential role for FGF signaling in the regulation of osteoblast function and bone growth, *Development 130*, 3063−3074.
5. Blobel, G. (1995) Soluble factors required for nuclear protein import, *Cold Spring Harbor Symp. Quant. Biol. 60*, 1−10.
6. Ibrahimi, O. A., Zhang, F., Hrstka, S. C., Mohammadi, M., and Linhardt, R. J. (2004) Kinetic model for FGF, FGFR, and proteoglycan signal transduction complex assembly, *Biochemistry 43*, 4724−4730.
7. Yeh, B. K., Eliseenkova, A. V., Plotnikov, A. N., Green, D., Pinnell, J., Polat, T., Gritli-Linde, A., Linhardt, R. J., and Mohammadi, M. (2002) Structural basis for activation of fibroblast growth factor signaling by sucrose octasulfate, *Mol. Cell. Biol. 22*, 7184−7192.
8. Pellegrini, L., Burke, D. F., Von Delft, F., Mulloy, B., and Blundell, T. L. (2000) Crystal structure of fibroblast growth factor receptor ectodomain bound to ligand and heparin, *Nature 407*, 1029−1034.
9. Hung, K. W., Kumar, T. K. S., Chi, Y. H., Chiu, I. M., and Yu, C. (2004) Molecular cloning, overexpression, and characterization of the ligand-binding D2 domain of fibroblast growth factor receptor, *Biochem. Biophys. Res. Commun. 317*, 253−258.
10. Prudovsky, I., Bagale, C., Tarantini, F., Mandinova, A., Soldi, R., Bellum, S., and Maciag, T. (2002) The intracellular translocation of the components of the fibroblast growth factor 1 release complex precedes their assembly prior to export, *J. Cell Biol. 158*, 201−208.
11. Prudovsky, I., Mandinova, A., Soldi, R., Bagala, C., Graziani, I., Landriscina, M., Tarantini, F., Duarte, M., Bellum, S., Doherty, H., and Maciag, T. (2003) The non-classical export routes: FGF1 and IL-1α point the way, *J. Cell Sci. 116*, 4871−4881.
12. Landriscina, M., Soldi, R., Bagala, C., Micucci, I., Bellum, S., Tarantini, F., Prudovsky, I., and Maciag, T. (2001) S100A13 participates in the release of fibroblast growth factor 1 in response to heat shock in vitro, *J. Biol. Chem. 276*, 22544−22552.
13. Jackson, A. A., Tarantini, S., Gamble, S., Friedman, S., and Maciag, T. (1995) The release of fibroblast growth factor-1 from NIH 3T3 cells in response to temperature involves the function of cysteine residues, *J. Biol. Chem. 270*, 29−36.
14. Landriscina, M., Bagalia, C., Mandinora, A., Soldi, R., Miccuci, I., Bellum, S., Prudovsky, I., and Maciag, T. (2001) Copper induces the assembly of a multiprotein aggregate implicated in the release of fibroblast growth factor 1 in response to stress, *J. Biol. Chem. 276*, 25549−25557.
15. Jahn, R., Lang, T., and Sudhoff, T. C. (2003) Membrane fusion, *Cell 112*, 519−529.
16. Fernandez-Chacon, R., Shin, O. H., Konigstorfer, A., Matos, M. F., Meyer, A. C., Garcia, J., Gerber, S. H., Rizo, J., Sudhof, T. C., and Rosenmund, C. (2002) Structure/function analysis of Ca^{2+} binding to the C2A domain of synaptotagmin 1, *J. Neurosci. 22*, 8438−8446.
17. Gerber, S. H., and Sudhof, T. C. (2002) Role of electrostatic and hydrophobic interactions in Ca^{2+}-dependent phospholipid binding by the C_2A-domain from synaptotagmin I, *Diabetes 51*, 3−11.
18. Hui, E., Bai, J., Wang, P., Sugimori, M., Llinas, R. R., and Chapman, E. R. (2005) Three distinct kinetic groupings of the synaptotagmin family: Candidate sensors for rapid and delayed exocytosis, *Proc. Natl. Acad. Sci. U.S.A. 102*, 5210−5214.
19. Bai, J., and Chapman, E. R. (2004) The C2 domains of synaptotagmin−Partners in exocytosis, *Trends Biochem. Sci. 29*, 143−151.
20. Marqueze, B., Berton, F., and Seagar, M. (2000) Synaptotagmins in membrane traffic: Which vesicles do the tagmins tag? *Biochemie 80*, 409−420.
21. Fuente, J. M., Eaton, P., Barrentos, A. G., Menendez, M., and Panades, S. (2005) Thermodynamic evidence for Ca^{2+}-mediated self-aggregation of Lewis X gold glyconanoparticles. A model for cell adhesion via carbohydrate-carbohydrate interaction, *J. Am. Chem. Soc. 127*, 6192−6197.
22. Gill, S. C., and von Hippel, P. H. (1989) Calculation of protein extinction coefficients from amino acid sequence data, *Anal. Biochem. 182*, 319−326.
23. Wohlgemuth, S., Kiel, C., Kramer, A., Serrano, L., Wittinghofer, F., and Herrmann, C. (2005) Recognizing and defining true Ras binding domains I: Biochemical analysis, *J. Mol. Biol. 348*, 741−758.
24. Gerber, S. H., Rizo, J., and Sudhof, T. C. (2002) Role of electrostatic and hydrophobic interactions in Ca^{2+}-dependent phospholipid binding by the C_2A-domain from synaptotagmin I, *Diabetes 51*, 512−518.
25. Huang, S. L., Lin, F. Y., and Yang, C. P. (2005) Microcalorimetric studies of the effects on the interactions of human recombinant interferon-α2a, *Eur. J. Pharm. Sci. 24*, 545−552.
26. Barney, B. M., Lobrutto, R., and Francisco, W. A. (2004) Characterization of a small metal binding protein from *Nitrosomonas europaea*, *Biochemistry 43*, 11206−11213.
27. Kayhani, J., Keyhani, E., Zarchipaurs, S., Tayefi Nasrabadi, H., and Einollathij, N. (2005) Stepwise binding of nickel to horseradish peroxidase and inhibition of the enzymatic activity, *Biochim. Biophys. Acta 1722*, 312−323.
28. Kraus, J., Bogner, E., Lilie, H., Eickmann, M., and Garten, W. (2005) Oligomerization and assembly of the matrix protein of Borna disease virus, *FEBS Lett. 579*, 2686−2692.
29. Zhang, X., Rizo, J., and Sudhof, T. C. (1998) Mechanism of phospholipid binding by the C2A-domain of synaptotagmin I, *Biochemistry 37*, 12395−12405.
30. Shao, X., Fernandez, I., Sudhof, T. C., and Rizo, J. (1998) Solution structures of the Ca^{2+}-free and Ca^{2+}-bound C2A domain of

synaptotagmin I: Does Ca^{2+} induce a conformational change? *Biochemistry 37*, 16106−16112.
31. Gai, D., Li, D., Finkelstein, C. V., Ott, R. D., Taneja, P., Fanning, E., and Chen, X. S. (2004) Insights into the oligomeric states, conformational changes, and helicase activities of SV40 large tumor antigen, *J. Biol. Chem. 279*, 38952−38957.
32. Fernandez-Chacon, R., Shin, O. H., Konigstrofer, A., Matos, M. F., Meyer, A. C., Garcia, J., Gerber, S. H., Rizo, J., Sudhof, T. C., and Rosenmund, C. (2002) Structure/function analysis of Ca^{2+} binding to the C2A domain of synaptotagmin 1, *J. Neurosci. 22*, 8438−8446.
33. Hajduk, P. J., Huth, J. R., and Fesik, S. W. (2005) Druggability indices for protein targets derived from NMR-based screening data, *J. Med. Chem. 48*, 2508−2525.
34. Bertini, I., Fragai, M., Lee, Y. M., Luchinat, C., and Terni, B. (2004) Paramagnetic metal ions in ligand screening: The Co(II) matrix metalloproteinase 12, *Angew. Chem., Int. Ed. 43*, 2254−2256.
35. Fernandez-Chacon, R., Konigstorfer, A., Gerber, S. H., Garcia, J., Matos, M. F., Stevens, C. F., Brose, N., Rizo, J., Rosermund, C., and Sudhof, T. C. (2001) Synaptotagmin I functions as a calcium regulator of release probability, *Neuron 410*, 41−49.
36. Chapman, E. R. (2002) Synaptotagmin: A Ca^{2+} sensor that triggers exocytosis? *Nat. Rev. Mol. Cell Biol. 3*, 498−508.
37. Wang, P., Wnag, C. T., Bai, T., Jackson, M. B., and Chapman, E. R. (2003) Mutations in the effector binding loops in the C2A and C2B domains of synaptotagmin I disrupt exocytosis in a nonadditive manner, *J. Biol. Chem. 278*, 47030−47037.
38. Ubach, J., Zhang, X., Shao, X., Sudhof, T. C., and Rizo, J. (1998) Ca^{2+} binding to synaptotagmin: How many Ca^{2+} ions bind to the tip of a C2-domain? *EMBO J. 17*, 3921−3940.
39. Rajini, B., Graham, C., Wistaon, G., and Sharma, Y. (2003) Stability, homodimerization, and calcium-binding properties of a single, variant $\beta\gamma$-crystallin domain of the protein absent in melanoma 1 (AIM1), *Biochemistry 42*, 4552−4559.
40. Evans, J. H., Gerber, S. H., Murray, D., and Leslie, C. C. (2004) The calcium binding loops of the cytosolic phospholipase A2 C2 domain specify targeting to Golgi and ER in live cells, *Mol. Biol. Cell 15*, 371−383.
41. Wilder, P. T., Varney, K. M., Weiss, M. B., Gitti, R. K., and Weber, D. J. (2005) S100B($\beta\beta$) inhibits the protein kinase C-dependent phosphorylation of a peptide derived from p53 in a Ca^{2+}-dependent manner, *Biochemistry 44*, 5690−5702.
42. Rustandi, R. R., Drohat, A. C., Baldiserri, D. M., Wilder, P. T., and Weber, D. J. (1998) The Ca^{2+}-dependent interaction of S100B-($\beta\beta$) with a peptide derived from p53, *Biochemistry 37*, 1951−1960.
43. Baudier, J., and Gerard, D. (1986) Ions binding to S100 proteins. II. Conformational studies and calcium-induced conformational changes in S100 $\alpha\alpha$ protein: The effect of acidic pH and calcium incubation on subunit exchange in S100a ($\alpha\beta$) protein, *J. Biol. Chem. 261*, 8204, 8212.
44. Bhattacharya, S., Large, E., Heizzmann, C. W., Hemmings, S., and Chazin, W. J. (2003) Structure of the Ca^{2+}/S100B/NDR kinase peptide complex: Insights into S100 target specificity and activation of the kinase, *Biochemistry 42*, 14416−14426.
45. Inman, K. G., Yang, R., Rsutandi, R. R., Miller, K. E., Baldisseri, D. M., and Weber, D. J. (2002) Solution NMR structure of S100B bound to the high-affinity target peptide TRTK-12, *J. Mol. Biol. 324*, 1003−1014.
46. Maroz, O. V., Anton, A. A., Grinst, S. J., Maitland, N. J., Dudson, G. G., Wilson, K. S., Lukanidin, E., and Bronstein, I. B. (2003) Structure of the human S100A12-copper complex: Implications for host-parasite defence, *Acta Crystallogr. B59*, 859−867.
47. Rae, T. D., Schmidt, P. J., Pufahl, R. A., Culotta, V. C., and O'Halloran, T. V. (1999) Undetectable intracellular free copper: The requirement of a copper chaperone for superoxide dismutase, *Science 284*, 805−808.
48. Harrison, M. D., Jones, C. E., and Damerson, C. T. (1999) Copper chaperones: Function, structure and copper-binding properties, *J. Biol. Inorg. Chem. 14*, 145−153.
49. Luk, E., Jensen, L. T., and Culotta, V. C. (2003) The many highways for intracellular trafficking of metals, *J. Biol. Inorg. Chem. 8*, 803−809.
50. Elmeskini, R., Culotta, V. C., Mains, R. E., and Eipper, B. A. (2003) Supplying copper to the cuproenzyme peptidylglycine α-amidating monooxygenase, *J. Biol. Chem. 278*, 12278−12284.
51. Koradi, R., Billeter, M., and Wuthrich, K. (1996) MOLMOL: A program for display and analysis of macromolecular structures, *J. Mol. Graphics 14*, 51−55.
52. Goddard, T. D., and Kneller, D. G. (2003) *SPARKY 3*, University of California, San Francisco.

BI051387R